JOURNAL OF MATERIALS SCIENCE **40** (2005) 1975–1978

Structural study on Al-26 mass% Si-8 mass% Ni powder

K. SAKSL
HASYLAB at Deutsches Elektronen Synchrotron, Notkesrtasse 85, 22607 Hamburg, Germany

J. ĎURIŠIN, M. OROLÍNOVÁ, K. ĎURIŠINOVÁ, P. LAZÁR
Institute of Materials Research, Slovak Academy of Science, Watsonova 47, 043 53, Košice, Slovak Republic

The structure of Al-26 mass% Si-8 mass% Ni alloy, a material used as an input product for manufacturing light weight products via powder metallurgy, was investigated by *in situ* powder diffraction techniques up to 700°C. Thermal expansion of the dominant phases indicates substitutional alloying of silicon by nickel atoms, forming a solid solution phase stable in the temperature region from 330 to 550°C. The presence of Al, Si, Al_3Ni and Si_3Ni was determined by phase analysis from a sample annealed at 700°C (re-melted) and cooled down to room temperature. EXAFS analysis of as prepared and re-melted samples documented similar local atomic structure around the Ni atoms in both stages.

1. Introduction

The hypereutectic aluminium-silicon alloys (Si > 20%) are characterised by low weight, high wear resistance, high dimensional stability and high strength at room and elevated temperatures. They are designated for parts in automotive engines and household electric appliances which are permanently exposed to temperatures ranging from 200 to 300°C, e.g. connecting rods, rotors, pistons, compressor components, gas turbine components, etc. [1]. Disadvantage of this alloys lies in the crystallization of the primary silicon phase over a wide temperature range, forming large particles with tendency to segregate inside the casted matrix. Such heterogeneous structural units embedded in a matrix are usually an interior source of stress or temperature induced defects resulting in a reduction of the mechanical properties and machineability of the alloy. This problem might be overcome by preparation of the materials via powder metallurgy (PM) techniques applying a gas atomisation process from the melts.

The AlSi alloys designed for high temperature applications in addition contain increased amounts of elements such a Ni, Fe, Cr, Mn, Ti, Zr, characterized by low diffusion coefficients and reduced equilibrium solid solubility in aluminium [2]. Their main task in the alloy is to increase the thermal stability of the aluminium matrix. However, using classical casting technology, the amounts of these elements should be relatively small (in order of 1 wt%). Higher amounts of the elements usually form a large, hard and brittle intermetallic phase deteriorating the mechanical properties of the alloy. Rapid solidification processes on the other hand permit to increase the amount of the alloying elements. The resulting intermetallic precipitates are small and equally distributed in the matrix and the above mentioned negative effect on the mechanical characteristics is negligible [2].

The Ni content in the PM hypereutectic AlSi alloy improves the mechanical properties (primarily toughness) and together with aluminium forms a fine-grained intermetallic Al_3Ni phase thermally stable up to ∼500°C [3]. The effectively small and equally dispersed Al_3Ni particles help strengthening grain boundaries of the matrix and suppressing its growth at elevated temperatures. Silicon-based dispersoids on the other hand, are essential to obtain a combination of a low thermal expansion and good strength properties, but their presence in the composition significantly reduces the formability of the final alloy. Therefore their content should not be too high. In general, intermetallic phases are most effective in the stabilisation of the Al matrix if they have a homogeneous and stable size distribution.

In this work, we present results of our measurements on Al-26 mass% Si-8 mass% Ni (AlSiNi) alloy originally designed for high temperature applications. The morphology and microstructure of as-prepared powder is documented by scanning electron microscopy (SEM) and optical microscopy, respectively. The structure evolution of the alloy gradually heated up to 700°C was investigated by *in situ* powder diffraction and possible changes in local atomic neighborhood around the Ni atoms of as-prepared and re-melted samples were monitored by EXAFS.

2. Experimental material and procedure

AlSiNi powder was produced under semi-industrial conditions by the Non-Ferrous Metals Institute, Light Metal Division in Skawina, Polland. Ingots of nominal compositions Al, Si, Ni 66, 26 and 8 mass%, respectively, were prepared by conventional casting from the melt. Those ingots as a technological precoursor for powder preparation were in the next stage re-melted, the melts atomizatied in conditions of compressed inert gas and the droplets subsequently cooled in water. After drying, the resulting powder was fractioned and the fraction below 150 μm was chosen as subject of our microstructural analyses.

The powder sample morphology and microstructure was examined by scanning electron microscopy (SEM) (Tesla BS 340 equiped with EDS microanalyser Link ISIS 300) and by optical microscopy (NEOPHOT 32).

In situ high temperature X-ray powder diffraction measurements were performed at HASYLAB/DESY on the experimental station Petra1. The XRD patterns of an AlSiNi powder sample were collected in a temperature range from 30 to 700°C, the later temperature being far above the melting point of the Al-based matrix. In practice, a quartz capillary filled by sample material was mounted in a capillary adapter allowing to keep the sample in vacuum $<10^{-5}$ mbar. Simultaneously, sample was heated (20°C/min) by a resistive heater designed for *in situ* measurements. The temperature was controlled by a thermocouple placed inside the capillary with the measuring point almost touching the free surface of the sample. More details about the equipment can be found in [4]. The gradually annealed sample was illuminated for 30 s for each pattern by X-rays of wavelength $\lambda = 0.5879$ Å. Two-dimensional XRD patterns were recorded by a fast area CCD detector (MarCCD 165). Sample detector distance, detector orthogonality with respect to the incoming radiation as well as precise radiation energy were determined by fitting a standard reference LaB_6 sample [5]. The images taken from different stages of annealing were integrated into 2Theta space by using Fit2D [6]. The Rietveld refinement method implemented in GSAS code [7] was used to fit the whole XRD patterns aiming to precisely (accuracy $\pm$ 0.002 Å) determine the lattice parameters of Si and Al phases.

Extended X-ray absorption fine structure (EXAFS) measurements above the Ni K-edge were performed at the E4 station (HASYLAB/DESY) in transmission geometry. The as prepared and re-melted (from powder diffraction experiment) powder sample was scanned in an energy range from 8080 to 8950 eV. The measured spectra were analyzed by standard procedures of data reduction, using the program Viper [8]. First the EXAFS signal, $\chi(k)$ was extracted and weighted by k^2 and a Kaiser-Bessel apodization function (coefficients $A = 12$, $\bar{k} = 7$), followed by Fourier transformation (FT) over the region where the amplitude of the non-weighted $\chi(k)$ is significant (for details see [8]). The FT gives a radial distribution function (RDF), modified by the phase shifts due to the absorbing and backscattering atoms. The contribution of the first shells only was backtransformed into k-space. The structural parameters N (coordination number), R (interatomic distance), and σ^2 (mean-square relative displacement, Debye-Waller factor) were obtained from least squares fitting in k-space, using theoretical phases and amplitude functions calculated by the FEFF-8 code [9].

3. Results and discussion

Fig. 1 shows a SEM picture of a AlSiNi powder sample. The typical spherical morphology and significant size distribution of particles is a characteristic feature of powders prepared by gas atomization process. Fig. 2 shows the microstructure of the powder particles documented by optical microscopy. The particular phases visible on the micrograph have been primarily identified by EDS analysis (not shown here). On the Fig. 2, the microstructure of the larger powder particles ~50 μm is formed by relatively coarse 1–6 μm silicon and fine $<1\mu$m intermetallics fractions embedded in Al-based solid solution matrix. A microstructure containing coarse silicon is usually not favorable. A large fraction of Si/matrix interface can be source of cracks, cavities, pores. Moreover the hard and brittle Si particles reduce machineability of the final products. The formation of the microstructure can be directly related to the cooling rate of melt droplets

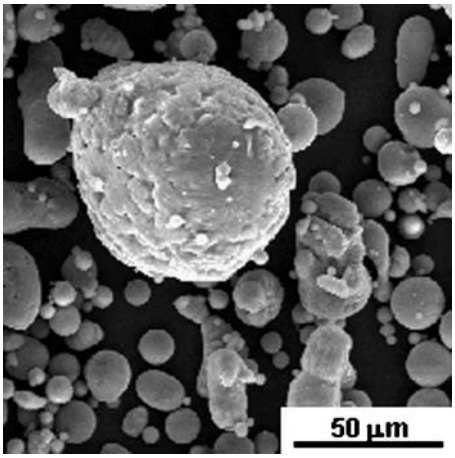

Figure 1 Scanning electron micrograph showing typical particle morphology AlSiNi powder sample.

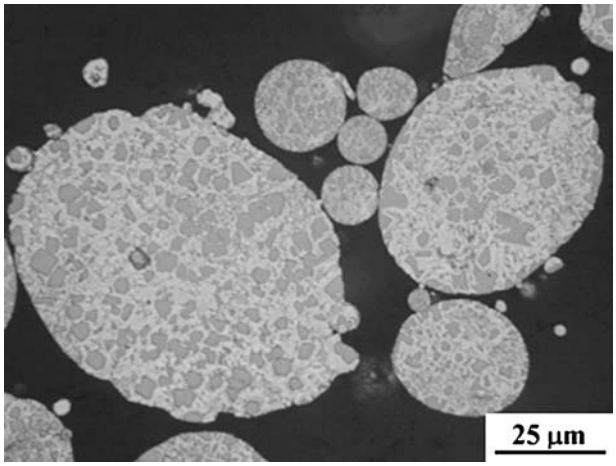

Figure 2 Optical microscopy micrographs showing microstructure of the AlSiNi powder sample.

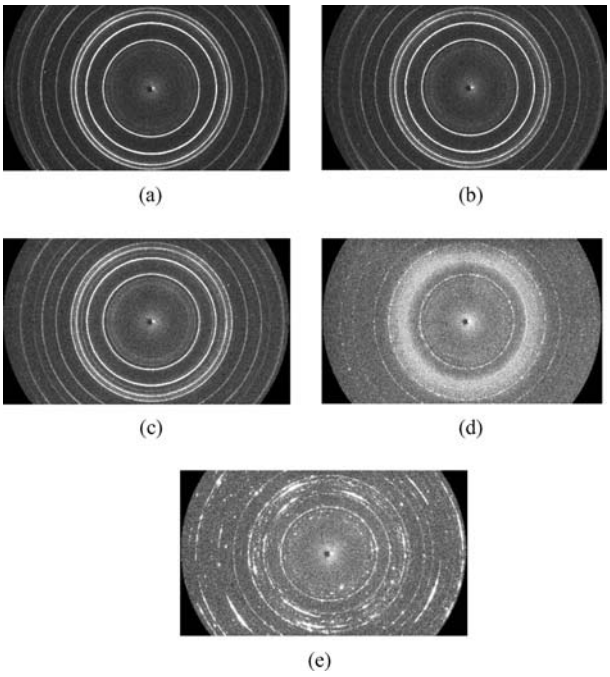

Figure 3 X-ray Two-Dimensional diffraction patterns taken from sample annealed at a. 30°C, b. 400°C, c. 570°C, d. 590°C and e. after cooling to room temperature from 700°C.

in the technology process. Following the same logic, the smaller particles ∼10 μm, seen at the same picture, show a much more distributed silicon fraction with diameter less than 1 μm.

Very important in the sense of following the thermodeformation processing of the powder as well as the resulting mechanical properties of the final solid product is to investigate the structural stability at higher temperatures. *In situ* X-ray powder diffraction is one of the most useful techniques giving a direct evidence of structure evolution at elevated temperatures. Fig. 3 shows selected 2D XRD patterns recorded at different the temperatures. The images taken at 30, 400 and 570°C show typical powder diffraction concentric Debye-Scherrer rings. On the other hand, the image taken from the sample annealed at 590°C is characterized by a diffuse hallo ring (centered round 14.95°) originating from the molten Al matrix, together with partially segmented silicon Debye-Scherrer rings. Fig. 4 shows the XRD patterns after radial integration from the corresponding images to 2Theta space. The major peaks exhibit systematic shifts towards to lower 2Theta values due to the expansion of the crystal lattice. Additional Bragg- peaks appear resulting from the formation of new phases at higher temperature. The plot clearly shows melting of the Al matrix above 570°C where reflections from the Al-phase disappeared while the reflections of the Si-phase are still present. Phase analysis was performed on the XRD pattern taken from the same sample annealed at 700°C and cooled down (by rate 20°C/min) to room temperature. Indexed phases are: Al (space group: $Fm\bar{3}m$; $a = 4.049$ Å), Si ($Fd\bar{3}m$; $a = 5.43$ Å), orthorhombic Al_3Ni (Pnma; $a = 6.611$ Å, $b = 7.366$ Å, $c = 4.811$ Å) and cubic Ni_3Si ($Pm\bar{3}m$; $a = 3.504$ Å).

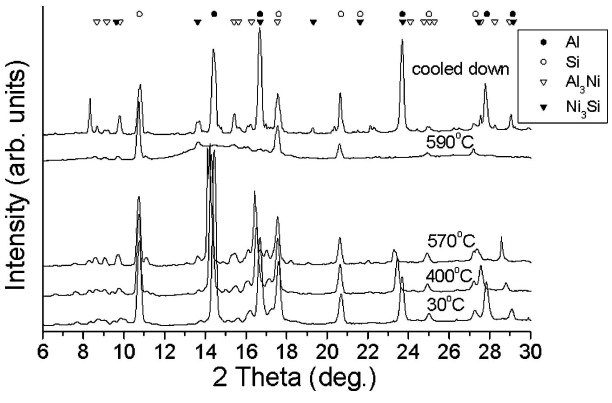

Figure 4 Integrated images shown in Fig. 3 converted into 2Theta space, Bragg's peaks of participating phases are marked.

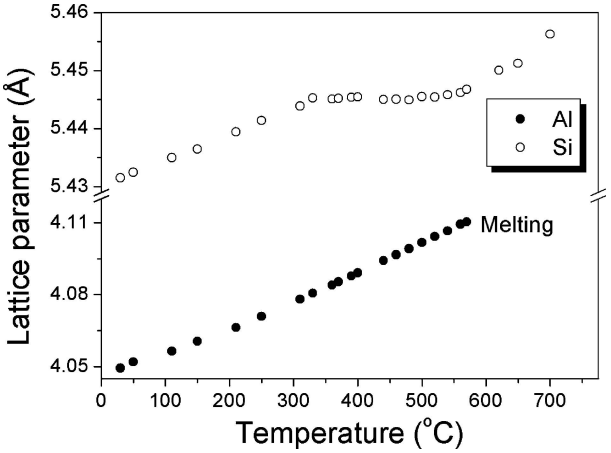

Figure 5 Lattice parameter expansion with temperature of a. Al and b. Si phases.

Interesting results brought analysis of Al and Si lattice expansions in dependence to annealing temperatures, Fig. 5. Aluminium shows linear increase of lattice parameter with temperature, while silicon linearly increasing up to 330°C and then the lattice parameter become almost constant up to 570°C. Significant increase of the parameters is seen again after the melting of Al-based matrix. One possible explanation for this extraordinary behavior might be diffusion of Ni atoms into the silicon lattice and substitution of Si atoms by nickel. The effective source of the Ni atoms can be Al-Ni solid solution as well as dissociated Al_3Ni phase. The thermal expansion of the Si lattice is compensated by substitution of larger Si atoms (radius 1.32 Å) by smaller Ni atoms (radius 1.24 Å). Such a Si-Ni solid solution appears to be stable up to the melting of Al-based matrix. During the Si-Ni atoms substitution, the Si atom may also be taking part of the Ni_3Si phase formation, as suggested in Fig. 4. At higher temperatures the Ni atoms diffuse back from solid solution to the melt where their solubility is higher. Consequentially, the Ni-less silicon phase lattice expanding as can be seen on Fig. 5 and above mentioned segmentation of Si Debye rings can be directly accounted to the growing of Si crystallites.

Of particular interest is the role of Ni in the composition. We performed EXAFS analysis of the as-prepared sample and the sample annealed at 700°C subsequently cooled down to room temperature (the same sample

TABLE I Fit values of local structural parameters around Ni atoms for AlSiNi alloy. R is the interatomic distance, N the coordination number, σ^2 the Debye-Waller factor

Sample	$R_{\text{Ni-Al}}$ (Å)	$N_{\text{Ni-Al}}$	$\sigma^2_{\text{Ni-Al}}$ ($\times 10^{-2}$ Å^2)
As prepared	2.4549 ± 0.0002	5.64 ± 0.01	0.010 ± 0.001
After melting	2.4509 ± 0.0002	5.50 ± 0.01	0.0064 ± 0.0008

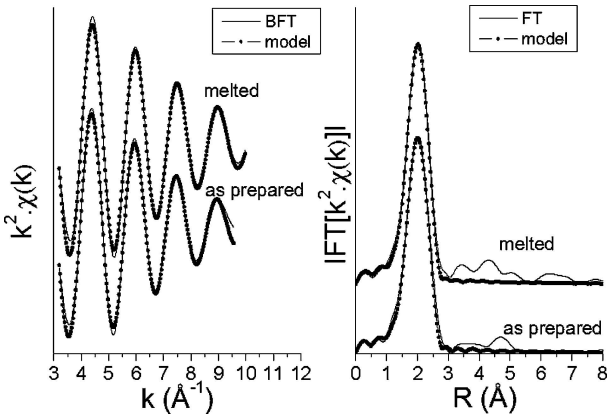

Figure 6 EXAFS spectra analysis of AlSiNi powder sample in as prepared and melted stages a. back Fourier transforms of first shell (solid line) together with fitted model (solid + symbol line), b. Fourier transforms (solid line) of normalized experimental EXAFS spectra together with model (solid + symbol line).

as in powder diffraction experiment) with the aim to investigate eventual changes in the short range order around Ni. Normalized experimental EXAFS spectra (not shown here) measured above the Ni-K edge were Fourier transformed (FT's) to R-space (see Fig. 6b, solid line) and only the first shell from 0 to 3 Å was back Fourier transformed (BFT) to k-space shown in Fig. 6a (solid line). The BFT's signals were in both cases fitted using theoretical phases and amplitude functions calculated from an arrangement of atoms in the ordered Al_3Ni phase by using the FEFF-8 code. The resulting fits are shown on Fig. 6a and b. We obtained the structural parameters listed in Table I for the Ni-Al pairs: interatomic distance R, coordination number N and Debye-Waller factor σ^2. The R and N parameters are practically identical proved similar local arrangement around Ni atoms for both of the material stages. Only mean-square relative displacement parameter for as prepared sample is significantly higher, what can be explained by presence of grain boundaries and other imperfection introduced to the matrix during preparation of the powder. The refined Ni-Al interatomic average distance 2.45 Å is smaller than simple sum of nominal atomic radii 2.68 Å, but in very good agreement with Ni-Al distance in orthorhombic Al_3Ni phase ($r_{\text{Ni-Al}_1} = 2.4218$ Å; $r_{\text{Ni-Al}_2} = 2.44523$ Å; $r_{\text{Ni-Al}_3} = 2.52098$ Å).

4. Summary

In summary, spherical morphology and significant size distribution of AlSiNi powder sample was shown by SEM. The microstructure of the powder particles in general consists of silicon and intermetallic compounds embedded in Al-based matrix.

In situ X-ray powder diffraction measurements show the structural evolution of AlSiNi powder sample at elevated temperatures. Melting of the Al-based matrix has been observed above 570°C while the Si phase proved to remain crystalline even at 700°C. Determined phases in the sample annealed at 700°C and cooled down to room temperature are: Al ($Fm\bar{3}m$; $a = 4.049$ Å), Si ($Fd\bar{3}m$; $a = 5.43$ Å), orthorhombic Al_3Ni ($Pnma$; $a = 6.611$ Å, $b = 7.3662$ Å, $c = 4.811$ Å) and cubic Ni_3Si ($Pm\bar{3}m$; $a = 3.504$ Å). Analysis of the lattice parameters shows a linear expansion of Al up to the melting and lattice parameter stabilization of Si in a temperature range between 330°C and 550°C. An explanation of this behavior can be found in substitutional alloying of Si by Ni and creation of a solid solution persisting up to the melting of Al-based matrix. Analysis of EXAFS spectra does not show any significant differences between the sample in the as-prepared state and after annealing at 700°C, indicating similar local atomic arrangements around Ni in both stages. Refined structural parameters are listed in Table I.

Acknowledgments

The authors would like to thank HASYLAB staff for support during the experiments. This work was supported by the European Commission and by the Government of Slovak Republic within the project G5RD-CT2000-00341.

References

1. P. SMITH, *Powder Metall.* **33** (1990) 202.
2. D. VOJTECH, J. MAIXNER, H. HEJDOVA, C. BARTA and C. JR. BARTA, *Kovove Mater.* **39** (2001) 149.
3. B. J. BAYLES, J. A. FORD and M. J. SALKIND, *Trans. AIME* **239** (1967) 844.
4. H. FRANZ, A. EHNES, A. ROGGENBUCK, K. SAKSL and G. WELLENREUTHER, *HASYLAB annual report* **1** (2002) 109.
5. NIST Standard Reference Material, SRM 660a.
6. A. P. HAMMERRSLEY, ESRF Internal Report, ESRF98HA01T, FIT2D V9.129 Reference Manual V3.1 (1998).
7. A. C. LARSON and R. B. VON DREELE, GSAS, general structure analysis system, report LAUR 86–748. Los Alamos: Los Alamos National Laboratory (1986).
8. K. V. KLEMENTIEV, *J. Phys. D: Appl. Phys.* **34** (2001) 209.
9. A. L. ANKUDINOV, B. RAVEL, J. J. REHR and S. D. CONRADSON, *Phys. Rev. B* **58** (1998) 7565.

Received 31 August
and accepted 24 September 2004